

1 **Kill and cure: genomic phylogeny and bioactivity of a diverse collection of *Burkholderia*  
2 *gladioli* bacteria capable of pathogenic and beneficial lifestyles**  
3

4 **Authors:**

5 Cerith Jones<sup>1,5</sup>, Gordon Webster<sup>1</sup>, Alex J. Mullins<sup>1</sup>, Matthew Jenner<sup>2,9</sup>, Matthew J. Bull<sup>1,6</sup>,  
6 Yousef Dashti<sup>2,7</sup>, Theodore Spilker<sup>3</sup>, Julian Parkhill<sup>4,8</sup>, Thomas R. Connor<sup>1</sup>, John J. LiPuma<sup>3</sup>,  
7 Gregory L. Challis<sup>2,9,10</sup> and Eshwar Mahenthiralingam<sup>1#</sup>

8

9 **Affiliations:**

10 <sup>1</sup> Microbiomes, Microbes and Informatics Group, Organisms and Environment Division, School  
11 of Biosciences, Cardiff University, Cardiff, Wales, CF10 3AX, UK

12

13 <sup>2</sup> Department of Chemistry, University of Warwick, CV4 7AL, UK

14

15 <sup>3</sup> Department of Pediatrics, University of Michigan Medical School, Ann Arbor, Michigan, USA.

16

17 <sup>4</sup> Wellcome Trust Sanger Institute, Wellcome Trust Genome Campus, Hinxton, Cambridge,  
18 CB10 1SA UK.

19

20 <sup>5</sup> Current address: School of Applied Sciences, Faculty of Computing, Engineering and  
21 Science, University of South Wales, Pontypridd, CF37 4BD, UK

22

23 <sup>6</sup> Current address: Pathogen Genomics Unit, Public Health Wales Microbiology Cardiff,  
24 University Hospital of Wales, Cardiff, CF14 4XW

25

26 <sup>7</sup> Current address: The Centre for Bacterial Cell Biology, Biosciences Institute, Medical School,  
27 Newcastle University, Newcastle upon Tyne, NE2 4AX, UK

28

29 <sup>8</sup> Current address: Department of Veterinary Medicine, Madingley Road, Cambridge, CB3 0ES

30

31 <sup>9</sup> Warwick Integrative Synthetic Biology Centre, University of Warwick, Coventry CV4 7AL, UK

32

33 <sup>10</sup> Department of Biochemistry and Molecular Biology, Biomedicine Discovery Institute,  
34 Monash University, Clayton, VIC 3800, Australia

35

36

37 **#Corresponding Author:** Prof. Eshwar Mahenthiralingam, Microbiomes, Microbes and  
38 Informatics Group, Organisms and Environment Division, School of Biosciences, Cardiff  
39 University, Sir Martin Evans Building, Room 2.06, Museum Avenue, Cardiff CF10 3AX, United  
40 Kingdom; Tel. +44 (0)29 20875875; Fax. +44 (0)29 20874305;  
41 Email: MahenthiralingamE@cardiff.ac.uk (ORCID: 0000-0001-9014-3790)

42

43 **Co-corresponding Author:** Cerith Jones, School of Applied Sciences, Faculty of Computing,  
44 Engineering and Science, University of South Wales, Pontypridd, CF37 4BD, United Kingdom,  
45 Tel. +44 (0)1443 654711

46 Email: cerith.jones@southwales.ac.uk (ORCID 0000-0001-6275-023)

47

48

49 **Running title:** Population genomics of *B. gladioli*

50

51

52 **Key words:** *Burkholderia*, *B. gladioli*, antibiotic production, plant pathogenesis, cystic fibrosis  
53 infection, phylogenomics.

54 **ABSTRACT**

55  
56 *Burkholderia gladioli* is one of few bacteria with a broad ecology spanning disease in humans,  
57 animals, and plants, and encompassing beneficial interactions with multiple eukaryotic hosts.  
58 It is a plant pathogen, a bongrekic acid toxin producing food-poisoning agent, and a lung  
59 pathogen in people with cystic fibrosis (CF). Contrasting beneficial traits include antifungal  
60 production exploited by insects to protect their eggs, plant protective abilities and antibiotic  
61 biosynthesis. We explored the ecological diversity and specialized metabolite biosynthesis of  
62 206 *B. gladioli* strains, phylogenomically defining 5 evolutionary clades. Historical disease  
63 pathovars (pv) *B. gladioli* pv. *allicola* and *B. gladioli* pv. *cocovenenans* were phylogenetically  
64 distinct, while *B. gladioli* pv. *gladioli* and *B. gladioli* pv. *agaricicola* were indistinguishable. Soft-  
65 rot disease and CF infection pathogenicity traits were conserved across all pathovars.  
66 Biosynthetic gene clusters for toxoflavin, caryoynencin and enacyloxin were dispersed across  
67 *B. gladioli*, but bongrekic acid and gladiolin production were clade specific. Strikingly, 13% of  
68 CF-infection strains characterised (n=194) were bongrekic acid toxin positive, uniquely  
69 linking this food-poisoning risk factor to chronic lung disease. Toxin production was  
70 suppressed by exposing strains to the antibiotic trimethoprim, providing a potential therapeutic  
71 strategy to minimise poisoning risk in CF.

72  
73 **INTRODUCTION**

74  
75 The genus *Burkholderia* contains important plant, animal and human pathogenic bacteria  
76 (Depoorter et al 2016, Lipuma 2010) as well as environmentally beneficial species (Suarez-  
77 Moreno et al 2012). Recently, amino acid and nucleotide based analyses have split  
78 *Burkholderia* strains into five distinct lineages corresponding to *Burkholderia* sensu stricto,  
79 *Paraburkholderia*, *Caballeronia*, *Robbsia*, *Trinickia* and *Mycetohabitans*, and a single species  
80 lineage represented by *Paraburkholderia rhizoxinica* (Estrada-de Los Santos et al 2018).  
81 Within *Burkholderia* sensu stricto, the *Burkholderia cepacia* complex group of species are  
82 problematic lung pathogens in people with cystic fibrosis (CF) (Lipuma 2010). The three most  
83 commonly isolated *Burkholderia* species among US CF patients are *B. multivorans*, *B.*  
84 *cenocepacia*, and interestingly, *B. gladioli* (Lipuma 2010). Although phenotypically similar,  
85 genetically *B. gladioli* is not a member of the *B. cepacia* complex, but is part of a group of  
86 species associated with plant disease including *B. glumae* and *B. plantarii* (Suarez-Moreno et  
87 al 2012). In relation to CF infection, *B. gladioli* may cause severe systemic abscesses (Jones  
88 et al 2001) and is also considered a risk factor for lung transplantation since it is associated  
89 with poor clinical outcome (Murray et al 2008). While the potential for patient-to-patient spread  
90 and rapid clinical decline are identified traits of *B. cepacia* complex infection in people with CF

91 (Lipuma 2010), the population biology, epidemiology and genomics of *B. gladioli* as a lung  
92 pathogen are essentially unknown.

93 In relation to its environmental ecology, *B. gladioli* was originally isolated as a pathogen of the  
94 *Gladiolus* genus of flowering plants and its taxonomy updated several times (Coenye et al  
95 1999). The current species encompasses the historical *Gladiolus*-disease causing taxa  
96 “*Pseudomonas gladioli*” and “*Pseudomonas marginata*” (Hildebrand et al 1973), the food  
97 poisoning-associated *B. cocovenenans* (Coenye et al 1999), and the potential biological  
98 control agent “*Pseudomonas antimicrobica*” (Coenye et al 2000). *B. gladioli* has also been  
99 isolated as a pathogen of important crops that resulted in pathovar (pv.) designations being  
100 applied to the causative isolates of: mushroom rot, *B. gladioli* pv. *agaricicola* (Gill and Tsuneda  
101 1997); onion rot, *B. gladioli* pv. *allicola* (Wright et al 1993); and the historical bulb rot disease,  
102 *B. gladioli* pv. *gladioli* (Hildebrand et al 1973). *B. gladioli* and its close relative *B. glumae* are  
103 also major rice pathogens causing panicle blight (Nandakumar et al 2009). *B. cocovenenans*  
104 represents a fourth pathovar (Jiao et al 2003) that is responsible for food poisoning when  
105 tempe bongrek, the fermented coconut-based Indonesian national dish, is produced with  
106 *Rhizopus* fungal cultures contaminated with *B. gladioli* (Moebius et al 2012). Under these  
107 conditions, a polyketide biosynthetic gene cluster (BGC) is activated resulting in *B. gladioli* pv.  
108 *cocovenenans* producing the respiratory toxin bongrekic acid that is fatal when ingested  
109 (Moebius et al 2012). The *B. gladioli* pathovars had been assigned based on the source of  
110 isolates and researchers have argued that there is a need to differentiate the lethal toxin  
111 producing pathovars such as *B. gladioli* pv. *cocovenenans* (Jiao et al 2003). However, the  
112 evolutionary basis of the pathovar designations of *B. gladioli* remains to be systematically  
113 investigated.

114  
115 The capacity to produce a diverse range of specialized metabolites ranging from toxins such  
116 as bongrekic acid (Moebius et al 2012) to beneficial antibiotics is a common trait among  
117 *Burkholderia* bacteria (Depoorter et al 2016, Kunakom and Eustaquio 2019). Close ecological  
118 associations with multiple eukaryotic hosts is a key primer for metabolite production by *B.*  
119 *gladioli*. As a detrimental trait, it produces the bright yellow phytotoxin, toxoflavin, which  
120 enhances the virulence of *B. gladioli* in rice disease (Lee et al 2016). In parallel with  
121 bongrekic acid biosynthesis, *B. gladioli* also produces the polyketide enacyloxin in co-culture  
122 with the fungus *Rhizopus microspores* (Ross et al 2014a). A close association of *B. gladioli*  
123 with fungi was linked to the discovery that the bacterium encodes a nonribosomal peptide  
124 synthetase BGC that produces icosalide A1, a metabolite originally characterised as a product  
125 of an *Aureobasidium* fungus (Dose et al 2018, Jenner et al 2019). PCR screening of DNA  
126 extracts from the original *Aureobasidium* culture demonstrated that a *B. gladioli* co-culture was

127 present (Jenner et al 2019). The vertical transmission of symbiotic *B. gladioli* in herbivorous  
128 *Lagriinae* beetles clearly demonstrates how ecological benefit may derive from the metabolites  
129 the bacterium produces (Florez et al 2017). *B. gladioli* was found in the reproductive tract of  
130 the beetles and resulted in the *Lagriinae* eggs gaining protection from fungal attack by the  
131 antimicrobial bacterial metabolites including toxoflavin, caryoynencin, the novel polyketide  
132 lagriene and novel aromatic glycoside sinapigladioside (Florez et al 2017).

133  
134 Genomics has revolutionized our understanding of *Burkholderia* population biology, and the  
135 beneficial and detrimental interactions of these ecologically diverse bacteria. The discovery of  
136 gladiolin, a novel polyketide antibiotic with promising activity against *Mycobacterium*  
137 *tuberculosis*, was greatly enhanced by complete genome sequencing of strain *B. gladioli*  
138 BCC0238 (Song et al 2017). Using a combination of systematic approaches including genome  
139 mining for specialized metabolite BGCs, metabolite characterisation and phenotypic assays,  
140 production of the antimicrobial cepacin was shown to underpin biological control of damping-  
141 off disease by the biopesticide species *Burkholderia ambifaria* (Mullins et al 2019). However,  
142 a limited number of complete genome sequences are available for *B. gladioli* which include  
143 those for strain BSR3, a rice disease isolate (Seo et al 2011), the bulb-associated Type strain  
144 ATCC 10248 (Johnson et al 2015), and the CF lung infection isolate, BCC0238 (Song et al  
145 2017). Here we investigate the population biology of *B. gladioli* as a functionally diverse  
146 species that interacts with human, plant, insect and microbial ecosystems. Using genome  
147 sequence analysis of 206 *B. gladioli* strains from diverse sources we defined the genetic  
148 linkage to pathovar status, mapped the ability to mediate plant soft-rot and human disease,  
149 and correlated population biology to capacity for specialized metabolite production. The  
150 genomics-based taxonomy of all the *B. gladioli* isolates was consistent with their designation  
151 as a single species. Pathovars *B. gladioli* pv. *allicola* and *B. gladioli* pv. *covenenans*, as well  
152 as biosynthetic clusters for bongrekic acid and gladiolin, were shown to be clade restricted  
153 within the overall *B. gladioli* population. People with CF were susceptible to all clades of *B.*  
154 *gladioli* and the presence of the bongrekic acid BGC was revealed as a new risk factor for  
155 these infectious isolates.

156  
157 **MATERIALS AND METHODS**

158  
159 **Bacterial strains and growth conditions**  
160 A collection of 206 *B. gladioli* isolates was assembled for this study and their source details,  
161 genomic features and the analysis they were subject to are included in supplementary data  
162 (Table S1). These were drawn from the Cardiff collection (Mahenthiralingam et al 2011,  
163 Mullins et al 2019, Song et al 2017) and *Burkholderia cepacia* Research Laboratory and

164 Repository (University of Michigan, Michigan, USA) (Lipuma 2010), with additional reference  
165 and pathovar strains of *B. gladioli* obtained from the Belgium Coordinated Collection of  
166 Microorganisms (Ghent, Belgium) and National Collections of Plant Pathogenic Bacteria  
167 (York, United Kingdom) (Table S1). *B. gladioli* isolates were routinely grown on Tryptone Soya  
168 Agar (TSA) or within Tryptone Soya Broth (TSB) liquid cultures, and incubated at 37°C.  
169 Antibiotic production was induced by growing strains on a minimal salts media with glycerol  
170 as the sole carbon source (designated Basal Salts Medium with Glycerol; BSM-G) as  
171 previously described (Hareland et al 1975, Mahenthiralingam et al 2011).

172  
173 Antimicrobial antagonism assays were performed by overlaying with the following  
174 susceptibility testing organisms: *Staphylococcus aureus* ATCC25923, *Ralstonia*  
175 *mannitolilytica* LMG6866, and *Candida albicans* SC 5314 as previously described  
176 (Mahenthiralingam et al 2011). *Escherichia coli* strain NCTC 12241 was used as a control for  
177 the mushroom and onion rot assays. Artificial CF sputum medium was made up as previously  
178 described (Kirchner et al 2012) to model if bongrekic acid production occurred under CF lung  
179 infection-like growth conditions. Trimethoprim (1 µg/mL) was incorporated into BSM-G to  
180 determine if *B. gladioli* metabolite production was induced by sub-inhibitory concentrations of  
181 this antibiotic as described for *B. thailandensis* (Okada et al 2016).

182  
183 **Genome sequencing, assembly and analysis**  
184 Genomic DNA was prepared from 3 mL TSB overnight cultures of *B. gladioli*. Cells were  
185 harvested by centrifugation and suspended in 400 µl of 4 M guanidine isothiocyanate solution  
186 (Invitrogen, UK). DNA was extracted from these bacterial suspensions using a Maxwell® 16  
187 automated nucleic acid purification system and the Maxwell® tissue DNA purification kit  
188 following the manufacturer's instructions (Promega, UK). Purified DNA extracts were treated  
189 with RNase (New England BioLabs, UK). Genomes were sequenced using the Illumina HiSeq  
190 2000 and HiSeq X Ten platforms at the Wellcome Sanger Institute as previously described  
191 (Mullins et al 2019). Genomes were assembled from the read data, annotated and compared  
192 using a virtual machine hosted by the Cloud Infrastructure for Microbial Bioinformatics (CLIMB)  
193 consortium (Connor et al 2016). Sequence reads were trimmed using Trim Galore v0.4.2  
194 (Babraham Bioinformatics), overlapped using FLASH v1.2.11 (Magoc and Salzberg 2011),  
195 and assembled using SPAdes v 3.9.1 (Bankevich et al 2012). Assembled genomes were  
196 polished using Pilon v1.21 (Walker et al 2014). Prokka v 1.12 beta (Seemann 2014) was used  
197 for gene prediction and annotation. The quality of genome assemblies was assessed using  
198 Quast (Gurevich et al 2013) and Prokka annotations cross-compared with gene predictions  
199 generated by Glimmer v3.02b (Delcher et al 2007). Draft genome contigs were ordered  
200 against a complete reference genome for *B. gladioli* BCC0238 (Song et al 2017) using

201 CONTUGuator v2.7 (Galardini et al 2011). To supplement the Illumina sequencing,  
202 contiguated genomes were generated for clade specific strains BCC1710, BCC1621 and  
203 BCC1622 (see Table S1) using Pacific Biosciences Single Molecule Real Time sequencing  
204 as described (Song et al 2017).

205

206 Average nucleotide identity (ANI) was used for genomic taxonomy and calculated using PyANI  
207 v0.2.1 (Pritchard et al 2016). The *B. gladioli* core genome was computed using Roary v3.6.0  
208 (Page et al 2015). Maximum-likelihood trees were drawn from the core gene alignment with  
209 FastTree (Price et al 2010) using the generalised time-reversible model of nucleotide evolution  
210 and visualised using FigTree (<http://tree.bio.ed.ac.uk/software/figtree>). Rooting the trees with  
211 multiple *Burkholderiales* species (*Burkholderia glumae*, *Burkholderia oklahomiensis* and  
212 *Paraburkholderia xenovorans*) failed to produce a biologically meaningful root. The closest  
213 sequences to these outgroups was variable but all produced trees of consistent phylogenetic  
214 separation for the *B. gladioli* clades identified. Therefore, an unrooted tree was presented in  
215 the final analysis. *B. gladioli* MLST sequence type assignments were made by using the  
216 PubMLST database and website (Jolley and Maiden 2010), via the MLST tool developed by  
217 Torsten Seemann (<https://github.com/tseemann/mlst>). Initial profiling of specialized metabolite  
218 biosynthetic gene potential was predicted for *B. gladioli* genomes via antiSMASH (Blin et al  
219 2017, Weber et al 2015) running as a local instance on CLIMB. The presence or absence of  
220 known BGCs was determined by mapping sequencing reads to representative BCG reference  
221 sequences using snippy (<https://github.com/tseemann/snippy>). Percentage of reads mapping  
222 to the reference sequence, and the actual number of corresponding reads were used to  
223 manually determine the status of each BGC in a given strain.

224

## 225 **Mushroom and onion rot bioassays**

226 Mushroom (*Agaricus bisporus*) soft-rot bioassays were carried out as described (Roy  
227 Chowdhury and Heinemann 2006) with the surface sterilisation and immersion into ice-cold  
228 water step omitted as this caused non-specific rotting of mushrooms. Briefly, mushrooms  
229 (Oakland closed cup mushroom, Lidl UK GmbH, produced in Ireland) were cut into 3-4 mm  
230 slices with a sterile blade. *B. gladioli* was grown overnight in TSB and the cap of each  
231 mushroom was inoculated with a 10 µl drop of bacterial suspension adjusted to 0.1 OD<sub>600 nm</sub>  
232 in TSB. Onion (*Allium cepa*) soft-rot bioassays were carried out as described (Jacobs et al  
233 2008). Brown onions (Tesco, Cardiff, UK) had their skin and outer onion layer removed prior  
234 to quartering with a sterile knife. Individual onion layers were cut into 3 to 4 cm pieces,  
235 wounded on their inner surface with a knife slit made under aseptic conditions, and the wound  
236 inoculated with 10 µl of bacterial suspension made as described for the mushroom assay. All  
237 assays (the test *B. gladioli*, a control *E. coli* NCTC 12241 strain, a TSB control and untreated

238 controls) were performed in triplicate on sterile wet filter paper contained in sterile 9 cm plastic  
239 Petri dishes, sealed with Parafilm M and incubated at 30°C for 48 h.

240

241 **Preparation of *B. gladioli* metabolite extracts and antimicrobial activity**

242 To analyse the metabolites produced by different *B. gladioli* strains, BSM-G agar plates (5 per  
243 strain) were streaked with cells from a freshly revived culture and incubated for 72 h at 30°C.  
244 Bacterial growth was removed using a sterile cell scraper and the spent agar was transferred  
245 to a glass bottle. Metabolites were extracted from the agar using dichloromethane (2 h with  
246 gentle shaking). The crude extract was concentrated to dryness under a vacuum at 22°C and  
247 resuspended in 1 mL of dichloromethane. The bioactivity of each extract and control  
248 dichloromethane was tested by pipetting 5 µL onto a TSA plate and allowing the plates to dry  
249 and solvent to evaporate. Each plate was then overlaid with molten Iso-sensitest agar (Oxoid,  
250 UK) seeded with *S. aureus*, *R. mannitolilytica* or *C. albicans* as described (Mahenthiralingam  
251 et al 2011). Plates were incubated at 37°C for 24 h and photographed to document the  
252 inhibitory zones of clearing observed. Bioactivity assays were performed in triplicate for each  
253 strain.

254

255 **Analysis of *B. gladioli* metabolites by high performance liquid chromatography (HPLC)**

256 HPLC analysis was used to quantify and identify known *B. gladioli* metabolites as follows.  
257 Specialized metabolites were induced using growth on BSM-G media (as above) and  
258 extracted directly from a 20 mm agar disc cut from the plates as described (Mullins et al 2019).  
259 Extracts (20 µL injection volume) were analysed on a Waters® AutoPurification™ HPLC  
260 System fitted with a reverse phase analytical column (Waters® XSelect CSH C18, 4.6 x 100  
261 mm, 5 µm) and a C18 SecurityGuard™ cartridge (Phenomenex) in series. Absorbance at 210-  
262 400 nm was monitored by a photo diode array detector (PDA). Mobile phases consisted of A:  
263 water with 0.1% formic acid and B: acetonitrile with 0.1% formic acid. A flow rate of 1.5 ml  
264 min<sup>-1</sup> was used. Elution conditions were as follows. 0-1 minutes: 95% A / 5% B; 1-9 minutes:  
265 gradient of A from 95 to 5% / gradient of B from 5% to 95%; 10-11 minutes: 5% A / 95% B;  
266 11-15 minutes: 95% A / 5% B. Peak height and area were calculated using MassLynx V4.1  
267 software ([www.waters.com](http://www.waters.com)).

268

269 To enable further biosynthetic pathway-metabolite correlations, *B. gladioli* gene mutants were  
270 used for the gladiolin BGC (Song et al 2017), and constructed *de novo* for the toxoflavin,  
271 bongrekic acid and caryoynencin pathways as follows. PCR products encoding fragments of  
272 core biosynthetic genes were amplified using specific primers (see Table S2) and cloned into  
273 the pGpΩTp suicide plasmid (Flannagan et al 2007) following digestion with *Xba*I/*Eco*RI (*bonA*  
274 and *cayA*), or *Xba*I/*Kpn*I (*toxA*). Plasmids were mobilised as described (Song et al 2017) and

275 mutants created in *B. gladioli* BCC0238 for the gladiolin and toxoflavin BGCs, strain BCC1710  
276 for the bongrekic acid BGC and strain BCC1697 for the caryoynencin pathway. Comparative  
277 analysis of metabolite extracts from parental versus mutant strains for each of the latter BGCs,  
278 together with correlation to mass spectrometry analysis (see below), was used to identify  
279 HPLC metabolite peaks.

280

## 281 **Culture conditions, extraction protocol and high-resolution mass spectrometry**

282 Known *Burkholderia* metabolites were confirmed by mass spectrometry essentially as  
283 described (Jenner et al 2019, Mahenthiralingam et al 2011, Mullins et al 2019, Song et al  
284 2017). Briefly, all *B. gladioli* strains were grown at 30 °C on BSM-G plates. Single plates were  
285 extracted by removal of the cell material, chopping of the agar and addition of 4 mL ethyl  
286 acetate for 2 h. Centrifugation in a 1.5 mL Eppendorf tube was used to remove debris. Crude  
287 extracts were directly analysed by UHPLC-ESI-Q-TOF-MS. UHPLC-ESI-Q-TOF-MS analyses  
288 were performed using a Dionex UltiMate 3000 UHPLC connected to a Zorbax Eclipse Plus C-  
289 18 column (100 × 2.1 mm, 1.8 µm) coupled to a Bruker MaXis II mass spectrometer. Mobile  
290 phases consisted of water (A) and acetonitrile (B), each supplemented with 0.1% formic acid.  
291 A gradient of 5 % B to 100 % B over 30 min was used at a flow rate of 0.2 ml min<sup>-1</sup>. The mass  
292 spectrometer was operated in either positive- or negative-ion mode with a scan range of 50–  
293 3,000 *m/z*. Source conditions were: end-plate offset at -500 V, capillary at -4,500 V, nebulizer  
294 gas (N<sub>2</sub>) at 1.6 bar, dry gas (N<sub>2</sub>) at 8 L min<sup>-1</sup> and dry temperature at 180 °C. Ion transfer  
295 conditions were: ion funnel radio frequency (RF) at 200 Vpp, multiple RF at 200 Vpp,  
296 quadrupole low mass at 55 *m/z*, collision energy at 5.0 eV, collision RF at 600 Vpp, ion cooler  
297 RF at 50–350 Vpp, transfer time at 121 µs and pre-pulse storage time at 1 µs. Calibration was  
298 performed with 1 mM sodium formate through a loop injection of 20 µl at the start of each run.

## 299 **PCR detection of the bongrekic Acid BGC**

300 To detect the presence of the bongrekic acid BGC, PCR probes were designed to target the  
301 central polyketide synthase enzyme gene, *bonA*, within the gene cluster of *B. gladioli*  
302 BCC1710 (*bonA*-F, 5' ATTTCTAGAAGTATCCGCATTTCGTCGC 3'; *bonA*-R 5'  
303 TATGAATTCGATCGATCAGTTGCGCTTCC 3'). PCRs were performed using the Taq PCR  
304 Core Kit (Qiagen) as per the manufacturer's instructions and incorporating Q-solution.  
305 Thermal cycling conditions used an annealing temperature of 54.5 °C and extension time of 1  
306 min 5 sec, run over 30 cycles. The 1053 bp *bonA* gene amplicon product was detected by gel  
307 electrophoresis and subjected to Sanger sequencing (Eurofins, Genomics) to confirm its  
308 identity from the control strain BCC1710.

309

## 310 **Accession Numbers**

311 The sequencing read data of *B. gladioli* isolates from this study are available from the  
312 European Nucleotide Archive under the project accession number PRJEB9765; isolate  
313 accession numbers are provided in Table S1.

314

## 315 RESULTS

316

### 317 Assembly and genomic taxonomy of a *B. gladioli* isolate collection

318 To provide a holistic understanding of taxonomy and pathovar population biology of *B. gladioli*,  
319 a representative collection of 206 isolates was assembled and their genomes sequenced  
320 (Table S1). The majority of isolates ( $n=194$ ) were from people with CF, with 181 from the USA,  
321 7 from the UK, 4 from Canada, and one each from Australia and Italy (Table S1). Twelve  
322 strains were from environmental sources including pathovar reference isolates as follows:  
323 isolates of plant-disease associated *B. gladioli* pv. *gladioli* ( $n=3$ ), pv. *agaricicola* ( $n=3$ ) and pv.  
324 *alliicola* ( $n=3$ ), and *B. gladioli* pv. *cocovenenans* ( $n=2$ ) reference toxin producing strains. One  
325 *B. gladioli* isolated from an environmental industrial source was also included (BCC1317;  
326 Table S1). Short read genome sequencing yielded high quality draft genomes (average of 82  
327 contigs, ranging from 20 [BCC1721] to 284 [BCC1788]) with a mean size for *B. gladioli* of 8.28  
328 Mb, GC content of 68% and encoding a mean of 6872 protein-encoding genes (Table 1).  
329 These metrics were consistent with previously reported *B. gladioli* genomes (Johnson et al  
330 2015, Seo et al 2011, Song et al 2017).

331

332 Since the assignment of isolates within the *Burkholderia* genus (Estrada-de Los Santos et al  
333 2018) generally, and *B. gladioli* specifically (Coenye et al 1999, Coenye et al 2000) have  
334 undergone multiple rounds of taxonomic re-classification, we initially established if the 206 *B.*  
335 *gladioli* isolates in the collection comprised a single bacterial species. Using average  
336 nucleotide identity, the 96.85% ANI for the entire *B. gladioli* 206 genome dataset was above  
337 the 95% identity required for designation as a single species (Goris et al 2007). This confirmed  
338 that the previous incorporation of “*P. cocovenenans*” (strains LMG 11626 and LMG 18113)  
339 (Coenye et al 1999) and “*P. marginata*” (ATCC10248) (Hildebrand et al 1973) into *B. gladioli*  
340 are supported by the genomic taxonomy (Goris et al 2007) (Table S1).

341

342 In addition, ANI heatmap analysis also suggested that a significant subspecies population  
343 structure existed within *B. gladioli* (Figure 1), and as such the following designation of groups  
344 was made. Group 1 ( $n=27$ ) comprised 3 closely related sub-groups: 1A, containing the  
345 reference *B. gladioli* pv. *cocovenenans* strains, 1B and 1C; each subgroup was distinct in  
346 terms of their ANI relatedness (Figure 1). All isolates within each subgroup encoded the  
347 bongrekic acid BGC (see below; Table S1) setting them apart from the rest of the *B. gladioli*

348 collection and supporting their collective designation as Group 1. Group 2 was composed of  
349 73 strains and included all 3 *B. gladioli* pv. *allicola* reference isolates. Group 3 ( $n = 106$ )  
350 contained both the *B. gladioli* pv. *agaricicola* and *B. gladioli* pv. *gladioli* reference isolates  
351 (Figure 1). Within each of these 3 initial groupings, the genomic ANI ranged from >98.1%  
352 (Group 3) to >99.1% (Group 1B), which was greater than the 96.85% collection average and  
353 suggested that distinct genetic lineages were present within *B. gladioli* (Figure 1).

354

355 **Core gene phylogenomic analysis reveals distinct evolutionary clades within *B. gladioli***  
356 To investigate the evolutionary linkages behind the ANI groupings (Figure 1), we constructed  
357 a phylogeny from the 4406 core genes identified within the 206 *B. gladioli* genome dataset.  
358 The strain groups defined by ANI (Figure 1) were also supported as distinct evolutionary  
359 clades in the phylogenomic analysis (Figure 2). The three Group 1 ANI sub-clusters  
360 correspondingly separated as clades 1A, 1B and 1C, with the reference *B. gladioli* pv.  
361 *cocovenenans* strains locating specifically to clade 1A (Figure 2). These Group 1 strains  
362 separated as 13 isolates in clade 1A, 4 in clade 1B and 10 isolates in clade 1C (Table S1). At  
363 the distal ends of the *B. gladioli* phylogenetic tree were clade 2 and clade 3 strains (Figure 2),  
364 that also corresponded exactly with the respective ANI groupings (Figure 1). All three  
365 reference *B. gladioli* pv. *allicola* strains mapped to clade 2 suggesting that this pathovar status  
366 was evolutionarily supported, but *B. gladioli* pv. *agaricicola* and pv. *gladioli* grouped within  
367 clade 3 and were not genetically distinguished (except that they were distinct from clades 1  
368 and 2; Figure 2).

369

370 **Ecological and disease associations of *B. gladioli* evolutionary clades**  
371 Given the evolutionary support for the clade restriction of *B. gladioli* pv. *allicola*, and grouping  
372 pathovars pv. *gladioli* and pv. *agaricicola* in a separate clade (Figure 2), the ability of selected  
373 *B. gladioli* strains to rot eukaryotic tissues was investigated. Mushroom soft-rot bioassays (Roy  
374 Chowdhury and Heinemann 2006) demonstrated that *B. gladioli* strains from all 3  
375 phylogenomic groups were capable of decaying mushroom tissue (Figure 3). The assay  
376 confirmed the ability of the pv. *agaricicola* reference strain NCPPB 3852 (BCC1883; Figure 3;  
377 panel K) to cause disease on its originally associated host. The degree of mushroom rot  
378 observed varied, with severe degradation of the mushroom cap tissue most apparent in clade  
379 2 and 3 strains, compared with clade 1 producing less extensive rot (Figure 3). The pathovar  
380 *agaricicola*-like strains therefore did not appear specifically adapted to degrade mushroom  
381 tissue. *B. gladioli* from all 3 clades also showed conserved plant tissue degradation capabilities  
382 within an onion soft-rot model (Jacobs et al 2008). A variable onion rot phenotype was  
383 observed for each strain, with the most extensive tissue pitting seen in clades 2 and clade 3

384 (Figure S1). Overall, rotting capability was demonstrated by the *B. gladioli* strains from all  
385 genetic groups.

386  
387 Since 94% of the 206 *B. gladioli* strain collection derived from CF lung infections (Table S1),  
388 this disease source was also the major origin for each of the evolutionary clades,  
389 demonstrating that opportunistic human pathogenicity was also a conserved species  
390 phenotype (Figure 2). For the 181 CF strains originating from the United States of America,  
391 mapping the state location of the submitting CF treatment centre showed that *B. gladioli*  
392 infections were geographically widespread with no phylogeographic linkages to clade types  
393 (Figure S2). The Group 1 *B. gladioli* strains (Figure 1 and 2) with the ability to produce  
394 bongrekic acid (see below) were also found to be capable of causing CF lung infections,  
395 linking them to opportunistic lung disease for the first time.

396  
397 ***B. gladioli* possess broad antimicrobial bioactivity**  
398 *B. gladioli* is known to produce an array of bioactive specialized metabolites including  
399 toxoflavin (Lee et al 2016), bongrekic acid (Moebius et al 2012), enacyloxins (Ross et al  
400 2014a), caryoynencin (Ross et al 2014b), sinapigladioside (Florez et al 2017), gladiolin (Song  
401 et al 2017), and icosalides (Dose et al 2018, Jenner et al 2019). Given this wealth of bioactive  
402 products, two *B. gladioli* strains representative of each clade within the species population  
403 biology (Figure 2) were screened for antimicrobial activity. Metabolite extracts from the spent  
404 agar of *B. gladioli* cultures were examined for their anti-Gram-positive, anti-Gram-negative,  
405 and antifungal activity respectively. All 10 strains tested demonstrated activity against *S.*  
406 *aureus*. Only the two isolates from *B. gladioli* clade 1C lacked antifungal activity, while the  
407 extracts from the *B. gladioli* clade 1C, clade 2 and clade 3 strains possessed anti-Gram-  
408 negative activity (Figure 4a). Overall, this antimicrobial activity analysis demonstrated that all  
409 the *B. gladioli* strains secreted extractable bioactive compounds, but the quantity and  
410 spectrum of bioactivity varied (Figure 4a).

411  
412 To determine which known metabolites accounted for the *B. gladioli* bioactivity (Figure 4b), a  
413 combination of HPLC, mass spectrometry and confirmatory BGC pathway mutagenesis was  
414 applied. Under the specialized metabolite inducing growth conditions used (Mahenthiralingam  
415 et al 2011), toxoflavin was found to be produced by all *B. gladioli* strains (Figure 4b). The  
416 isothiocyanate sinapigladioside (Florez et al 2017) was produced by both clade 1C strains and  
417 one clade 3 strain. Enacyloxin Ila (Mahenthiralingam et al 2011) was present in both clade 1A  
418 strains, a clade 1C strain, a clade 3 strain, and was also detected at low quantities within the  
419 clade 2 strain BCC1848 (Figure 4b). Production of the polyyne caryoynencin (Ross et al  
420 2014b) was widespread and detected in eight of the 10 strains tested, with an absence in the

421 clade 1C strains (Figure 4b). Gladiolin (Song et al 2017) was detected in its discovery strain  
422 *B. gladioli* BCC0238, but the macrolide was not present in other strains. Bongrekic acid was  
423 detected in all 6 clade 1 strains, although only limited amounts were present in the two clade  
424 1B strains examined (Figure 4b). Overall, the metabolite analysis showed that individual *B.*  
425 *gladioli* strains were capable of producing up to 4 different bioactive metabolites (Figure 4b)  
426 underpinning the broad spectrum of antimicrobial activity of *B. gladioli* (Figure 4a).

427

428 **Distribution of known specialized metabolite BGCs in *B. gladioli***

429 To expose the genetic basis of bioactivity and the production of multiple metabolites (Figure  
430 4), the distribution of known metabolite BGCs was mapped by genome mining. Using  
431 sequence read mapping to known *B. gladioli* BGCs the presence of toxoflavin, caryoynencin,  
432 bongrekic acid, enacyloxin, gladiolin, and icosalide BGCs were determined. Across the  
433 phylogenomically defined *B. gladioli* clades, random distribution as well as clade-specific  
434 presence of BGCs was observed (Figure 5a). The capacity for toxoflavin, caryoynencin and  
435 icosalide biosynthesis was widely distributed across *B. gladioli*, with the toxoflavin BGC being  
436 absent in only two of the 206 strains. The caryoynencin BGC was uniquely absent in all 10  
437 clade 1C strains (correlating to a lack of detection of the metabolite; Figure 4b). The icosalide  
438 BGC mirrored this clade 1C absence, but also showed random loss in six other strains from  
439 across *B. gladioli* (one clade 1B, four clade 2 and one clade 3 strains; Figure 5a). The gladiolin  
440 and bongrekic BGCs demonstrated evolutionary restrictions to specific clades as follows. A  
441 total of 83 of the 106 clade 3 strains (78%) encoded the gladiolin BGC and it was absent from  
442 the other *B. gladioli* clades. All 27 strains within clades 1A, 1B and 1C, encoded the BGC for  
443 bongrekic acid production, validating its presence as marker to collectively designate them  
444 as Group 1 *B. gladioli* strains (Figure 1), despite their distinct nature as evolutionary clades  
445 (Figure 2).

446

447 The enacyloxin BGC was randomly distributed within *B. gladioli* (Figure 5a). Its presence  
448 within clade 1 strains was most conserved with 21 of 27 strains (77%) being enacyloxin BGC  
449 positive and 100% of clade 1C strains encoding it. Interestingly, no strain within the collection  
450 of 206 encoded both the enacyloxin and gladiolin BGC (Figure 5a). Genomic interrogation of  
451 this inverse correlation led to the discovery that these large polyketide BGCs occupied the  
452 same genetic locus within *B. gladioli* when present (Figure 5b). This conserved region of the  
453 genome was on the second genomic replicon of *B. gladioli* and either encoded enacyloxin (43  
454 strains) or gladiolin (83 strains) or remained empty in terms of specialized metabolite BGCs  
455 (80 strains). Upstream and downstream of these polyketide BGC island insertion points were  
456 blocks of conserved and syntenic genomic DNA. These surrounding regions of the *B. gladioli*

457 second genomic replicon did not show the presence of mobile DNA markers to indicate the  
458 BGC insertion point acted as a gene capture hotspot.

459

460 ***B. gladioli* bongrekic acid biosynthesis: a new potential risk factor for CF lung**  
461 **infection**

462 In total, 25 of the 27 strains within clades 1A, 1B and 1C, were recovered from CF infection  
463 (Table S1 and Figure 2), and all possessed the bongrekic acid BGC (Figure 5A). To date this  
464 lethal toxin has only been associated with food poisoning related *B. gladioli* (Gudo et al 2018,  
465 Jiao et al 2003, Moebius et al 2012) and not linked to disease in people with CF. Analysis of  
466 12 toxin BGC positive strains showed that 11 of them produced bongrekic acid *in vitro*, but  
467 the extent of toxin production by each was variable (Figure S4). Four of these bongrekic acid  
468 producers (BCC1675, BCC1686, BCC1701 and BCC1710; Figure S4) were subsequently  
469 grown in artificial CF sputum medium (Kirchner et al 2012), and with the exception of strain  
470 BCC1701 (a low producer; Figure S4), toxin production was detected in the remaining 3 strains  
471 by LC-MS. This toxin production under CF lung infection-like growth conditions, prompted the  
472 development of diagnostic PCR probes to enable rapid identification of the bongrekic acid  
473 positive *B. gladioli* as a potential clinical risk marker for CF. Testing of this *bonA* gene (Moebius  
474 et al 2012) targeting PCR (Figure S6) on 122 of the *B. gladioli* CF strains prior to their genome  
475 sequencing identified 13 isolates as positive. Subsequent genome sequencing demonstrated  
476 that all encoded a complete BGC for the toxin (Figure 5a) validating the risk marker PCR.

477

478 Since CF patients are administered multiple antibiotics to suppress their lung infections. A  
479 recent finding that low concentrations of antibiotics may act as inducers of *Burkholderia*  
480 specialized metabolites (Seyedsayamdst 2014) added further potential risk to the occurrence  
481 of bongrekic toxin positive *B. gladioli* strains within CF individuals. Furthermore, the antibiotic  
482 trimethoprim, which is widely used for treatment of *Burkholderia* CF infections, was specifically  
483 shown to be a highly effective elicitor of specialized metabolite production in *B. thailandensis*  
484 (Okada et al 2016), compounding the threat of toxin activation. To test antibiotic induced BGC  
485 expression (Okada et al 2016, Seyedsayamdst 2014), six *B. gladioli* CF strains possessing  
486 a range of bongrekic acid production levels (Figure 6a) were screened for toxin production  
487 with and without the presence of sub-inhibitory levels of trimethoprim. In contrast to the *B.*  
488 *thailandensis* metabolite activation (Okada et al 2016), no *B. gladioli* strains demonstrated  
489 induction of bongrekic acid by exposure to trimethoprim, but five of the six strains analysed  
490 showed a clear suppression of toxin production (*B. gladioli* BCC1678, Figure 6b and 6c; Figure  
491 S6 shows the data for all six strains tested).

492

493 **DISCUSSION**

494 In the last decade the specialized metabolites produced by *Burkholderia* have been  
495 extensively studied and multiple compounds have been shown to be activated or functional in  
496 different ecological settings (Kunakom and Eustaquio 2019). *B. gladioli* shows a very wide  
497 range of beneficial (Coenye et al 2000, Florez et al 2017, Song et al 2017) versus detrimental  
498 traits (Coenye et al 1999, Gudo et al 2018, Hildebrand et al 1973, Jiao et al 2003, Quon et al  
499 2011), several of which relate to specialized metabolite production.  
500 With multiple taxonomic re-classifications (Coenye et al 1999, Coenye et al 2000), an  
501 unknown basis for pathovar status in plant disease (Coenye et al 1999, Hildebrand et al 1973,  
502 Wright et al 1993), calls for a specific recognition of the lethal food-poisoning "cocovenenans"  
503 pathovar (Jiao et al 2003), an emerging presence in CF lung infection (Lipuma 2010), and its  
504 expanding role as a source of specialized metabolites (Dose et al 2018, Jenner et al 2019,  
505 Kunakom and Eustaquio 2019, Ross et al 2014a, Ross et al 2014b, Song et al 2017), there  
506 was a clear need to understand the population ecology of *B. gladioli*.

507  
508 The ability of individual strains of *B. gladioli* to produce both beneficial or toxic specialized  
509 metabolites is also very interesting given their wide interactions with different eukaryotic hosts  
510 (Florez et al 2017, Lee et al 2016). Based on the ANI-genomic species concept (Goris et al  
511 2007), our novel genomic analyses confirmed that all pathovars of *B. gladioli* collectively  
512 comprise a single species. However, from the phylogenomic analysis, we have uniquely  
513 shown that *B. gladioli* comprises 5 evolutionarily distinct clades (Figure 2). The capacity to  
514 encode and produce the bongrekic acid toxin was specific to 3 of these clades (1A, 1B and  
515 1C) and provided a unifying, and potentially medically relevant feature to designate them as a  
516 single group. These bongrekic acid positive strains were also linked for the first time as a  
517 potential risk factor for people with CF. While production of the toxin during infection and its  
518 association with poor disease outcome needs to be determined, we have showed that toxin  
519 BGC is biosynthetically active in Group 1 *B. gladioli* strains recovered from people with CF  
520 (Figure S4).

521  
522 The population biology and pathogenicity traits of very few *Burkholderia* species has been  
523 described in depth using phylogenomics. The transmission dynamics of a *Burkholderia dolosa*  
524 CF outbreak was tracked in 14 patients over 16 years and identified mutations in the 112  
525 isolates that showed parallel evolution towards increased antibiotic resistance and tolerance  
526 of low oxygen (Lieberman et al 2011). The cause of melioidosis, *Burkholderia pseudomallei*,  
527 has been subjected to arguably the most extensive genomic characterisation because of its  
528 pathogenicity and due to its threat as a bioterrorism agent (Chewapreecha et al 2017).  
529 Genome sequencing of 469 *B. pseudomallei* isolates showed the species comprised two  
530 distinct populations, an ancestral Australian reservoir that anthropogenically transmitted and

531 diverged within Asia, and spread further via the slave trade from Africa to South America  
532 (Chewapreecha et al 2017). Mapping the phylogenomics of *B. ambifaria* as a historically used  
533 biopesticide revealed the BGC for cepacin A, a key antimicrobial mediating plant protection  
534 against pathogenic oomycetes (Mullins et al 2019). However, the population biology of plant  
535 pathogenic *Burkholderia* has not been studied in depth and our genomic analysis of *B. gladioli*  
536 is unique in uncovering whether plant pathovar status has an evolutionary basis. Only the *B.*  
537 *gladioli* pv. *allicola* associated with onion soft-rot plant disease were evolutionarily distinct as  
538 clade 2 strains (Figure 2), but rotting capability was associated with all clades and historical  
539 pathovars (Figure 3 and Figure S1). The specific genetic factors linked to the separation of  
540 pathovar *allicola* as clade 2 and its distinction from clade 3 plant disease strains remain to be  
541 determined.

542  
543 In contrast to the broad conservation of plant disease traits across *B. gladioli*, bongrekic acid  
544 producing strains (Gudo et al 2018, Jiao et al 2003, Moebius et al 2012) associated with fatal  
545 human food poisoning were more closely related. They were designated Group 1 by their ANI  
546 relatedness (Figure 1) and unifying bongrekic acid BGC presence (Figure 5). Although the  
547 human disease Group 1 *B. gladioli* pv. *cocovenenans* strains were not a distinct species  
548 (Figure 1) and occupied 3 distinct evolutionary clades (Figure 2), this 100% bongrekic acid  
549 BGC positivity adds weight to the call for their differentiation as a distinct toxin-positive *B.*  
550 *gladioli* subgroup (Jiao et al 2003). With 13% of the *B. gladioli* CF isolates examined encoding  
551 the bongrekic acid BGC, this is a worrying potential risk factor for *Burkholderia* lung  
552 infections, especially since toxin production can occur under lung infection-like growth  
553 conditions, such as artificial CF sputum. The clinical outcome of *Burkholderia* infection is  
554 frequently highly variable (Frangolias et al 1999) and severe systemic disease has been  
555 associated with *B. gladioli* in CF (Jones et al 2001). With the ability to rapidly identify  
556 bongrekic acid positive *B. gladioli* using a PCR diagnostic (Figure S5), we are now in a strong  
557 position to understand if the toxin plays a role in poor clinical outcome of infected CF patients.  
558 Also, since we have shown that trimethoprim acts to suppress toxin production (Figure 6),  
559 rather than activate this *Burkholderia* specialized metabolite (Kirchner et al 2012), a case can  
560 be made for antibiotic therapy to be maintained in bongrekic acid positive *B. gladioli* CF  
561 infection.

562  
563 By combining genomics with analytical chemistry, we have also been able to map the  
564 repertoire of bioactive specialized metabolite BGCs across the *B. gladioli* as a species. This  
565 demonstrated that the bioactivity of *B. gladioli* is frequently the result of the production of  
566 multiple metabolites (Figure 4). The widespread distribution and conservation of BGCs for  
567 toxoflavin (Lee et al 2016), caryoynencin (Ross et al 2014b) and the icosalides (Dose et al

568 2018, Jenner et al 2019) suggest they are ancestral to *B. gladioli* as a species (Figure 5). The  
569 specificity of gladiolin biosynthesis to clade 3 strains also sheds light on the classification of  
570 the recently identified symbiotic *B. gladioli* strains that protect the eggs of Lagriinae beetles  
571 from fungal attack (Florez et al 2017). The symbiotic beetle *B. gladioli* strain Lv-StA encodes  
572 the BGC for the antibiotic lagriene (Florez et al 2017) which identical to the BGC for the  
573 macrolide gladiolin (Song et al 2017). Since the gladiolin BGC, and by default the lagriene  
574 BGC, is restricted to *B. gladioli* clade 3, the insect symbionts must be members of this clade.  
575 It is also clear that all *B. gladioli* clades are geographically widely distributed from the analysis  
576 of US CF infection strains (Figure S2). The ecological significance of herbivorous Lagriinae  
577 and other beetles in distributing the such bacterial symbionts across continental ranges will  
578 be fascinating to understand.

579  
580 Within this study, we were able to gain an insight into the ecological distribution of *B. gladioli*  
581 by sampling the opportunistic infections the bacterium causes in people with CF. In the  
582 absence of patient-to-patient or common source transmission, the natural environment is the  
583 main source of *Burkholderia* CF lung infections (Lipuma 2010). From the US CF patient data  
584 (Figure S2), all *B. gladioli* clades appear widely distributed across a continental range. Soil,  
585 the rhizosphere and terrestrial freshwater environments are common sources of *Burkholderia*  
586 (Suarez-Moreno et al 2012). Outside of CF infection (Lipuma 2010), plant disease (Coenye et  
587 al 1999, Hildebrand et al 1973, Wright et al 1993) or food-poisoning (Jiao et al 2003), little is  
588 known about other sources of *B. gladioli*. Recent findings of close associations with insects  
589 (Florez et al 2017) and fungi (Dose et al 2018, Jenner et al 2019) point to multiple symbiotic  
590 roles *B. gladioli* may have in the natural environment. The population biology, pathogenicity,  
591 metabolite and BGC analysis we have carried out provides a systematic framework upon  
592 which the ecological distribution of *B. gladioli* can be mapped.

593

#### 594 **ACKNOWLEDGEMENTS**

595 This research was supported by a grant from the BBSRC (BB/L021692/1) to E.M, G.L.C,  
596 T.R.C and J.P; A.J.M., G.W. and E.M also acknowledged current funding from grant  
597 BB/S007652/1. E.M. and G.W. acknowledge funding from the Life Science Bridging Fund  
598 LSBF R2-004 for the HPLC analysis and instrumentation. T.R.C and M.J.B acknowledge  
599 funding from the MRC (MR/L015080/1). The Bruker MaXis II instrument used in this study was  
600 funded by the BBSRC (BB/M017982/1). M.J. is supported by a BBSRC Future Leader  
601 Fellowship (BB/R012121/1) and G.L.C. is the recipient of a Wolfson Research Merit Award  
602 from the Royal Society (WM130033).

603

604 **AUTHOR CONTRIBUTIONS** (CRediT taxonomy; <https://casrai.org/credit/>)

605 We describe author contributions to the paper using the CRedit taxonomy. *Conceptualisation*:  
606 E.M, and C.J.; *Data Curation*: E.M., C.J., G.W., A.J.M., M.J., J.P., J.J.L., and G.L.C.; *Formal*  
607 *analysis*: E.M., C.J., A.J.M., M.J., Y.D., J.P., J.J.L., and G.L.C; *Funding Acquisition*: E.M., J.P.,  
608 G.L.C. and J.J.L.; *Investigation*: E.M., C.J., G.W., A.J.M., M.J., J.P., T.S., J.J.L., and G.L.C;  
609 *Methodology*: C.J., G.W., A.J.M., M.J., Y.D., M.J.B., and T.R.C.; *Project Administration*: E.M.,  
610 J.P. and G.L.C; *Resources*: E.M., J.P., J.J.L., and G.L.C.; *Software*: C.J., A.J.M., M.J.B., and  
611 T.R.C.; *Supervision*: E.M., J.P. and G.L.C.; *Validation*: E.M., C.J; *Visualisation*: C.J., G.W. and  
612 E.M.; *Writing-Original Draft*: E.M. and C.J.; *Writing-Review & Editing*: all authors.  
613

## 614 CONFLICT OF INTEREST

615 No conflicts of interest are declared in relation to this research.  
616

## 617 REFERENCES

618  
619 Bankevich A, Nurk S, Antipov D, Gurevich AA, Dvorkin M, Kulikov AS *et al* (2012). SPAdes: a new  
620 genome assembly algorithm and its applications to single-cell sequencing. *J Comput Biol* **19**: 455-477.

621  
622 Blin K, Medema MH, Kottmann R, Lee SY, Weber T (2017). The antiSMASH database, a comprehensive  
623 database of microbial secondary metabolite biosynthetic gene clusters. *Nucleic Acids Res* **45**: D555-  
624 d559.

625  
626 Chewapreecha C, Holden MT, Vehkala M, Valimaki N, Yang Z, Harris SR *et al* (2017). Global and regional  
627 dissemination and evolution of *Burkholderia pseudomallei*. *Nat Microbiol* **2**: 16263.

628  
629 Coenye T, Holmes B, Kersters K, Govan JR, Vandamme P (1999). *Burkholderia cocovenenans* (van  
630 Damme *et al.* 1960) Gillis *et al.* 1995 and *Burkholderia vandii* Urakami *et al.* 1994 are junior synonyms  
631 of *Burkholderia gladioli* (Severini 1913) Yabuuchi *et al.* 1993 and *Burkholderia plantarii* (Azegami *et al.*  
632 1987) Urakami *et al.* 1994, respectively. *Int J Syst Bacteriol* **49 Pt 1**: 37-42.

633  
634 Coenye T, Gillis M, Vandamme P (2000). *Pseudomonas antimicrobica* Attafuah and Bradbury 1990 is a  
635 junior synonym of *Burkholderia gladioli* (Severini 1913) Yabuuchi *et al.* 1993. *Int J Syst Evol Microbiol*  
636 **50 Pt 6**: 2135-2139.

637  
638 Connor TR, Loman NJ, Thompson S, Smith A, Southgate J, Poplawski R *et al* (2016). CLIMB (the Cloud  
639 Infrastructure for Microbial Bioinformatics): an online resource for the medical microbiology  
640 community. *Microbial Genomics* **2**: doi:10.1099/mgen.1090.000086.

641  
642 Delcher AL, Bratke KA, Powers EC, Salzberg SL (2007). Identifying bacterial genes and endosymbiont  
643 DNA with Glimmer. *Bioinformatics* **23**: 673-679.

644

- 645 Depoorter E, Bull MJ, Peeters C, Coenye T, Vandamme P, Mahenthiralingam E (2016). *Burkholderia*:  
646 an update on taxonomy and biotechnological potential as antibiotic producers. *Appl Microbiol*  
647 *Biotechnol* **100**: 5215-5229.
- 648  
649 Dose B, Niehs SP, Scherlach K, Florez LV, Kaltenpoth M, Hertweck C (2018). Unexpected Bacterial  
650 Origin of the Antibiotic Icosalide: Two-Tailed Depsipeptide Assembly in Multifarious *Burkholderia*  
651 Symbionts. *ACS Chem Biol* **13**: 2414-2420.
- 652  
653 Estrada-de Los Santos P, Palmer M, Chavez-Ramirez B, Beukes C, Steenkamp ET, Briscoe L *et al* (2018).  
654 Whole Genome Analyses Suggests that *Burkholderia* sensu lato Contains Two Additional Novel Genera  
655 (*Mycetohabitans* gen. nov., and *Trinickia* gen. nov.): Implications for the Evolution of Diazotrophy and  
656 Nodulation in the *Burkholderiaceae*. *Genes (Basel)* **9**: 10.3390/genes9080389.
- 657  
658 Flannagan RS, Aubert D, Kooi C, Sokol PA, Valvano MA (2007). *Burkholderia cenocepacia* requires a  
659 periplasmic HtrA protease for growth under thermal and osmotic stress and for survival in vivo. *Infect*  
660 *Immun* **75**: 1679-1689.
- 661  
662 Florez LV, Scherlach K, Gaube P, Ross C, Sitte E, Hermes C *et al* (2017). Antibiotic-producing symbionts  
663 dynamically transition between plant pathogenicity and insect-defensive mutualism. *Nat Commun* **8**:  
664 15172.
- 665  
666 Frangolias DD, Mahenthiralingam E, Rae S, Raboud JM, Davidson AG, Wittmann R *et al* (1999).  
667 *Burkholderia cepacia* in cystic fibrosis. Variable disease course. *Am J Respir Crit Care Med* **160**: 1572-  
668 1577.
- 669  
670 Galardini M, Biondi EG, Bazzicalupo M, Mengoni A (2011). CONTIGuator: a bacterial genomes finishing  
671 tool for structural insights on draft genomes. *Source Code Biol Med* **6**: 11.
- 672  
673 Gill WM, Tsuneda A (1997). The interaction of the soft rot bacterium *Pseudomonas gladioli* pv  
674 *agaricicola* with Japanese cultivated mushrooms. *Can J Microbiol* **43**: 639-648.
- 675  
676 Goris J, Konstantinidis KT, Klappenbach JA, Coenye T, Vandamme P, Tiedje JM (2007). DNA-DNA  
677 hybridization values and their relationship to whole-genome sequence similarities. *Int J Syst Evol*  
678 *Microbiol* **57**: 81-91.
- 679  
680 Gudo ES, Cook K, Kasper AM, Vergara A, Salomao C, Oliveira F *et al* (2018). Description of a Mass  
681 Poisoning in a Rural District in Mozambique: The First Documented Bongrekic Acid Poisoning in  
682 Africa. *Clin Infect Dis* **66**: 1400-1406.
- 683  
684 Gurevich A, Saveliev V, Vyahhi N, Tesler G (2013). QUAST: quality assessment tool for genome  
685 assemblies. *Bioinformatics (Oxford, England)* **29**: 1072-1075.
- 686

- 687 Harelard WA, Crawford RL, Chapman PJ, Dagley S (1975). Metabolic function and properties of 4-  
688 hydroxyphenylacetic acid 1-hydroxylase from *Pseudomonas acidovorans*. *J Bacteriol* **121**: 272-285.
- 689
- 690 Hildebrand DC, Palleroni NJ, Doudoroff M (1973). Synonymy of *Pseudomonas gladioli* Severini 1913  
691 and *Pseudomonas marginata* (McCulloch 1921) Stapp 1928. *Int J Syst Evol Microbiol* **23**: 433-437.
- 692
- 693 Jacobs JL, Fasi AC, Ramette A, Smith JJ, Hammerschmidt R, Sundin GW (2008). Identification and onion  
694 pathogenicity of *Burkholderia cepacia* complex isolates from the onion rhizosphere and onion field  
695 soil. *Appl Environ Microbiol* **74**: 3121-3129.
- 696
- 697 Jenner M, Jian X, Dashti Y, Masschelein J, Hobson C, Roberts DM *et al* (2019). An unusual *Burkholderia*  
698 *gladioli* double chain-initiating nonribosomal peptide synthetase assembles 'fungal' icosalide  
699 antibiotics. *Chem Sci* **10**: 5489-5494.
- 700
- 701 Jiao Z, Kawamura Y, Mishima N, Yang R, Li N, Liu X *et al* (2003). Need to differentiate lethal toxin-  
702 producing strains of *Burkholderia gladioli*, which cause severe food poisoning: description of *B. gladioli*  
703 pathovar *cocovenenans* and an emended description of *B. gladioli*. *Microbiol Immunol* **47**: 915-925.
- 704
- 705 Johnson SL, Bishop-Lilly KA, Ladner JT, Daligault HE, Davenport KW, Jaissle J *et al* (2015). Complete  
706 genome sequences for 59 *Burkholderia* isolates, both pathogenic and near neighbor. *Genome*  
707 *Announc* **3**: 10.1128/genomeA.00159-00115.
- 708
- 709 Jolley KA, Maiden MC (2010). BIGSdb: Scalable analysis of bacterial genome variation at the population  
710 level. *BMC Bioinformatics* **11**: 595.
- 711
- 712 Jones AM, Stanbridge TN, Isalska BJ, Dodd ME, Webb AK (2001). *Burkholderia gladioli*: Recurrent  
713 abscesses in a patient with cystic fibrosis. *Journal of Infection* **42**: 69-71.
- 714
- 715 Kirchner S, Fothergill JL, Wright EA, James CE, Mowat E, Winstanley C (2012). Use of artificial sputum  
716 medium to test antibiotic efficacy against *Pseudomonas aeruginosa* in conditions more relevant to the  
717 cystic fibrosis lung. *J Vis Exp*: e3857.
- 718
- 719 Kunakom S, Eustaquio AS (2019). *Burkholderia* as a Source of Natural Products. *J Nat Prod* **82**: 2018-  
720 2037.
- 721
- 722 Lee J, Park J, Kim S, Park I, Seo YS (2016). Differential regulation of toxoflavin production and its role  
723 in the enhanced virulence of *Burkholderia gladioli*. *Mol Plant Pathol* **17**: 65-76.
- 724
- 725 Lieberman TD, Michel JB, Aingaran M, Potter-Bynoe G, Roux D, Davis MR, Jr. *et al* (2011). Parallel  
726 bacterial evolution within multiple patients identifies candidate pathogenicity genes. *Nat Genet* **43**:  
727 1275-1280.
- 728

- 729 Lipuma JJ (2010). The changing microbial epidemiology in cystic fibrosis. *Clin Microbiol Rev* **23**: 299-  
730 323.
- 731
- 732 Magoc T, Salzberg SL (2011). FLASH: fast length adjustment of short reads to improve genome  
733 assemblies. *Bioinformatics* **27**: 2957-2963.
- 734
- 735 Mahenthiralingam E, Song L, Sass A, White J, Wilmot C, Marchbank A *et al* (2011). Enacyloxins are  
736 products of an unusual hybrid modular polyketide synthase encoded by a cryptic *Burkholderia*  
737 *ambifaria* Genomic Island. *Chem Biol* **18**: 665-677.
- 738
- 739 Moebius N, Ross C, Scherlach K, Rohm B, Roth M, Hertweck C (2012). Biosynthesis of the respiratory  
740 toxin bongrekic acid in the pathogenic bacterium *Burkholderia gladioli*. *Chem Biol* **19**: 1164-1174.
- 741
- 742 Mullins AJ, Murray JAH, Bull MJ, Jenner M, Jones C, Webster G *et al* (2019). Genome mining identifies  
743 cepacin as a plant-protective metabolite of the biopesticidal bacterium *Burkholderia ambifaria*. *Nat*  
744 *Microbiol* **4**: 996-1005.
- 745
- 746 Murray S, Charbeneau J, Marshall BC, LiPuma JJ (2008). Impact of *burkholderia* infection on lung  
747 transplantation in cystic fibrosis. *Am J Respir Crit Care Med* **178**: 363-371.
- 748
- 749 Nandakumar R, Shahjahan AKM, Yuan XL, Dickstein ER, Groth DE, Clark CA *et al* (2009). *Burkholderia*  
750 *glumae* and *B. gladioli* Cause Bacterial Panicle Blight in Rice in the Southern United States. *Plant Dis*  
751 **93**: 896-905.
- 752
- 753 Okada BK, Wu Y, Mao D, Bushin LB, Seyedsayamdst MR (2016). Mapping the Trimethoprim-Induced  
754 Secondary Metabolome of *Burkholderia thailandensis*. *ACS Chem Biol* **11**: 2124-2130.
- 755
- 756 Page AJ, Cummins CA, Hunt M, Wong VK, Reuter S, Holden MT *et al* (2015). Roary: rapid large-scale  
757 prokaryote pan genome analysis. *Bioinformatics* **31**: 3691-3693.
- 758
- 759 Price MN, Dehal PS, Arkin AP (2010). FastTree 2--approximately maximum-likelihood trees for large  
760 alignments. *PLoS One* **5**: e9490.
- 761
- 762 Pritchard L, Glover RH, Humphris S, Elphinstone JG, Toth IK (2016). Genomics and taxonomy in  
763 diagnostics for food security: soft-rotting enterobacterial plant pathogens. *Analytical Methods* **8**: 12-  
764 24.
- 765
- 766 Quon BS, Reid JD, Wong P, Wilcox PG, Javer A, Wilson JM *et al* (2011). *Burkholderia gladioli* - a  
767 predictor of poor outcome in cystic fibrosis patients who receive lung transplants? A case of locally  
768 invasive rhinosinusitis and persistent bacteremia in a 36-year-old lung transplant recipient with cystic  
769 fibrosis. *Can Respir J* **18**: e64-65.
- 770

- 771 Ross C, Opel V, Scherlach K, Hertweck C (2014a). Biosynthesis of antifungal and antibacterial  
772 polyketides by *Burkholderia gladioli* in coculture with *Rhizopus microsporus*. *Mycoses* **57 Suppl 3**: 48-  
773 55.
- 774
- 775 Ross C, Scherlach K, Kloss F, Hertweck C (2014b). The molecular basis of conjugated polyyne  
776 biosynthesis in phytopathogenic bacteria. *Angew Chem Int Ed Engl* **53**: 7794-7798.
- 777
- 778 Roy Chowdhury P, Heinemann JA (2006). The general secretory pathway of *Burkholderia gladioli* pv.  
779 *agaricicola* BG164R is necessary for cavity disease in white button mushrooms. *Appl Environ Microbiol*  
780 **72**: 3558-3565.
- 781
- 782 Seemann T (2014). Prokka: rapid prokaryotic genome annotation. *Bioinformatics* **30**: 2068-2069.
- 783
- 784 Seo YS, Lim J, Choi BS, Kim H, Goo E, Lee B *et al* (2011). Complete genome sequence of *Burkholderia*  
785 *gladioli* BSR3. *J Bacteriol* **193**: 3149.
- 786
- 787 Seyedsayamdst MR (2014). High-throughput platform for the discovery of elicitors of silent bacterial  
788 gene clusters. *Proc Natl Acad Sci U S A* **111**: 7266-7271.
- 789
- 790 Song L, Jenner M, Masschelein J, Jones C, Bull MJ, Harris SR *et al* (2017). Discovery and Biosynthesis of  
791 Gladiolin: A *Burkholderia gladioli* Antibiotic with Promising Activity against *Mycobacterium*  
792 *tuberculosis*. *J Am Chem Soc* **139**: 7974-7981.
- 793
- 794 Suarez-Moreno ZR, Caballero-Mellado J, Coutinho BG, Mendonca-Previato L, James EK, Venturi V  
795 (2012). Common features of environmental and potentially beneficial plant-associated *Burkholderia*.  
796 *Microb Ecol* **63**: 249-266.
- 797
- 798 Walker BJ, Abeel T, Shea T, Priest M, Aboueliel A, Sakthikumar S *et al* (2014). Pilon: an integrated tool  
799 for comprehensive microbial variant detection and genome assembly improvement. *PLoS One* **9**:  
800 e112963.
- 801
- 802 Weber T, Blin K, Duddela S, Krug D, Kim HU, Brucolieri R *et al* (2015). antiSMASH 3.0-a comprehensive  
803 resource for the genome mining of biosynthetic gene clusters. *Nucleic Acids Res* **43**: W237-243.
- 804
- 805 Wright PJ, Clark RG, Hale CN (1993). A Storage Soft-Rot of New-Zealand Onions Caused by  
806 *Pseudomonas-Gladioli* Pv Alliicola. *New Zeal J Crop Hort* **21**: 225-227.
- 807

**Table 1.** Summary genome sequencing statistics

	<i>Mean</i>	<i>Maximum</i>	<i>Minimum</i>
<i>Number of Contigs</i>	82.6	284 (BCC1788)	20 (BCC1721)
<i>Genome Size</i>	8.28 Mb	8.94 Mb (BCC1815)	7.32 Mb (BCC1681)
<i>N50</i>	404821	1964774 (BCC1691)	147146 (BCC1713)
<i>%GC</i>	68.0 %	68.31 % (BCC1823)	67.39 % (BCC1815)
<i>Number of genes</i>	6872	7693	6012

## FIGURES

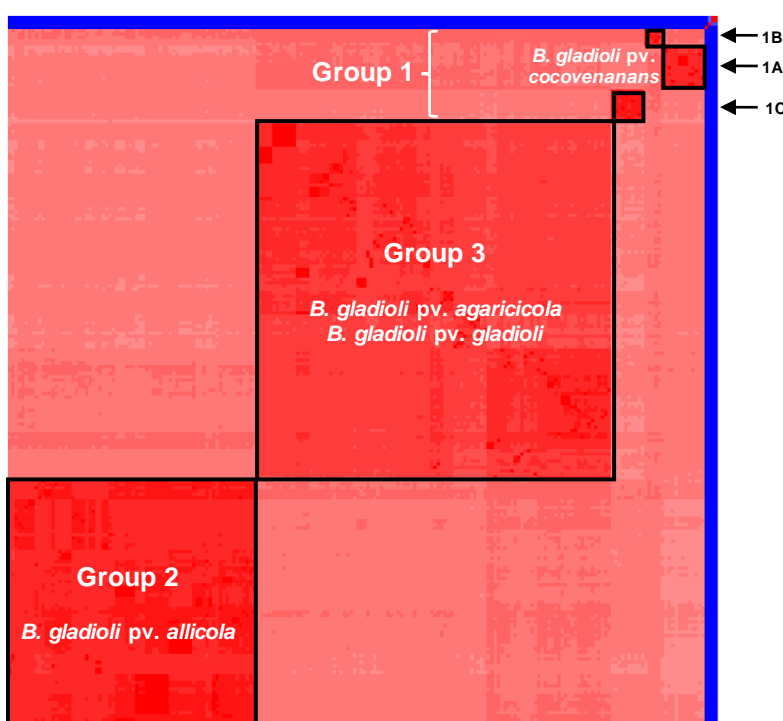


**Figure 1.** *B. gladioli* comprises a single genomic species with evidence of subspecies clustering by average nucleotide identity. The ANI of 206 *B. gladioli* genomes was compared using pyANI and a heatmap constructed (see methods). Darker red shading correlates to the greater percentage identity of each isolate. Subgroups with greater than 98.8% ANI are shown within the black outlined boxes. The main clusters are labelled as Group 1, 2 and 3, with Group 1 isolates sub-dividing further into sub-groups 1A, 1B and 1C (see top right). Four non-*B. gladioli* species genomes were used as taxonomic controls: 3 strains of the closely related species *B. glumae* and 1 strain of *B. ambifaria*; their low nucleotide identity to *B. gladioli* (ANI < 95%) is shown in blue.

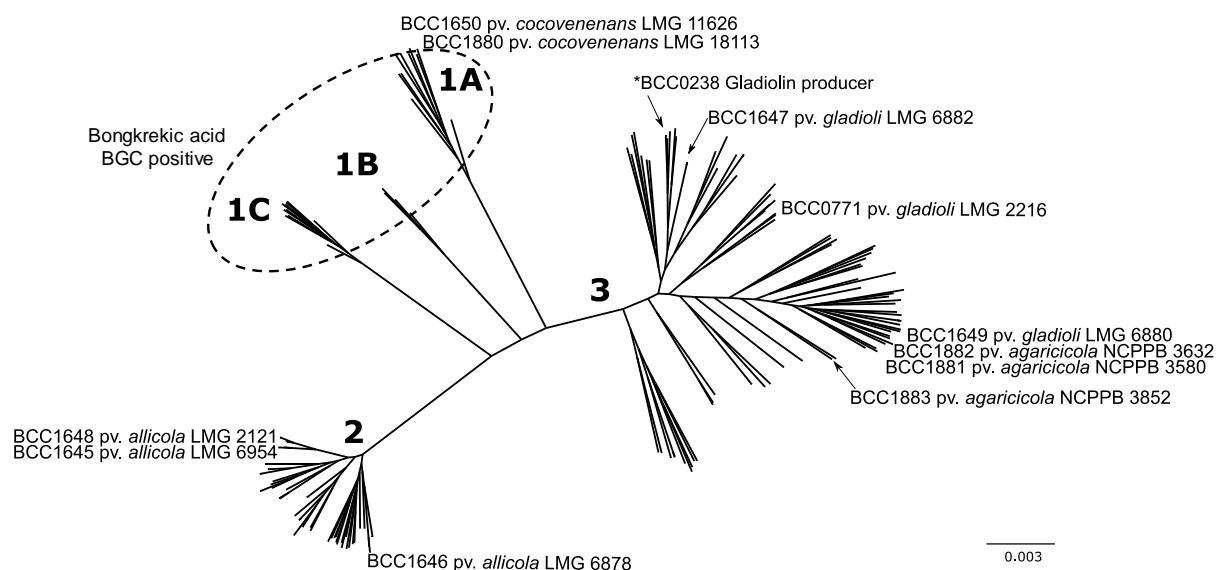


**Figure 2. The population biology of *B. gladioli* inferred by core genome gene phylogeny.** The core genome of the 206 *B. gladioli* strains were analysed using Roary and the resulting 4406 core genes aligned and used to construct a phylogeny. A maximum-likelihood un-rooted tree was constructed using the generalised time-reversible model of nucleotide evolution; multiple rooting with species outside of *B. gladioli* was used to confirmed topology (see materials and methods). The position of the *B. gladioli* plant pathovar reference strains and model gladiolin-producing strain, BCC0238 is shown. The 5 major evolutionary branches consistent with the ANI groups and sub-groups are numbered accordingly. Clades 1A,1B and 1C all encoded the bongrekic acid biosynthetic gene cluster as shown by the dashed oval and were collectively designated as Group 1 *B. gladioli*. The scale bar represents the number of base substitutions per site.

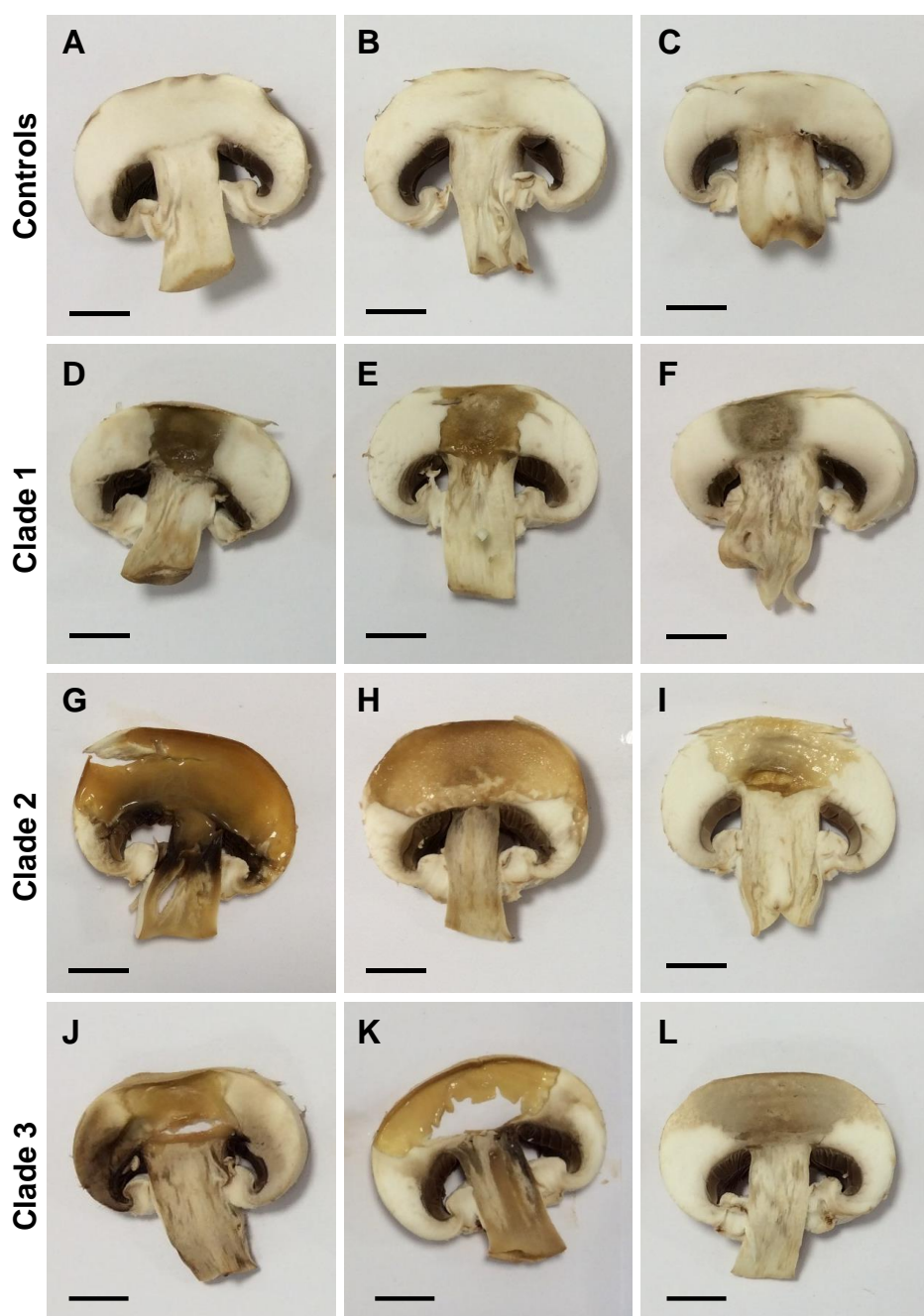
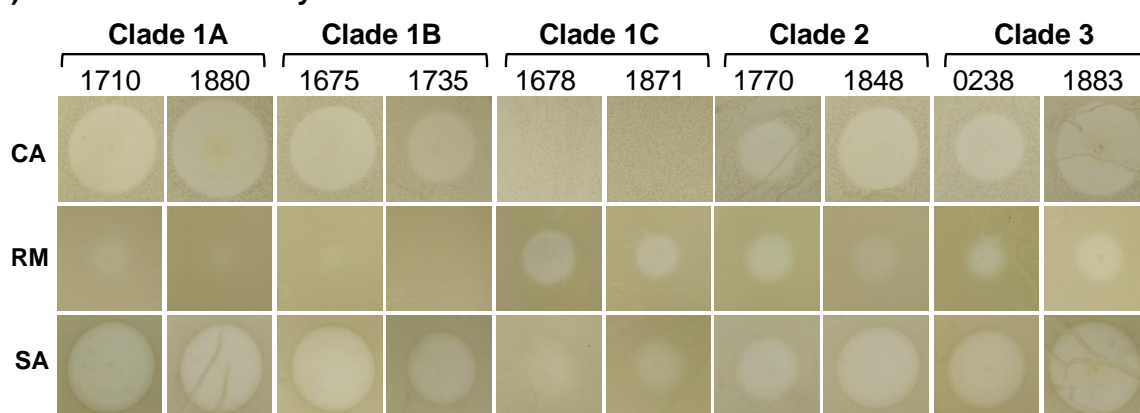


**Figure 3. *B. gladioli* from all evolutionary clades are capable of mushroom rot.** The ability of *B. gladioli* strains to degrade mushroom tissue was tested by inoculating commercial mushroom tissue slices with standardized bacterial cultures. Inoculated mushrooms were incubated at 30°C for 48 hours with the following shown in each panel (each row are either controls or *B. gladioli* clades as indicated on the left): (A) No treatment control, (B) TSB only, (C) *E. coli* NCTC 12241, (D) *B. gladioli* Clade 1A strain BCC1710, (E) Clade 1B strain BCC1675, (F) Clade 1C strain BCC1678, (G) *B. gladioli* Clade 2 strain BCC1731, (H) *B. gladioli* pv. *allicola* reference Clade 2 strain BCC1645, (I) *B. gladioli* pv. *allicola* reference Clade 2 strain BCC1646, (J) *B. gladioli* Clade 3 strain BCC0238, (K) *B. gladioli* pv. *agaricola* reference Clade 3 strain BCC1883 (NCPPB 3852), (L) *B. gladioli* pv. *gladioli* reference Clade 3 strain BCC771 (LMG 2216<sup>T</sup>). Pitting and tissue degradation was apparent in all *B. gladioli* inoculated mushrooms; a scale bar (1 cm) is shown in each panel to enable comparison.

**(A) Antimicrobial activity**



**(B) Metabolite analysis**

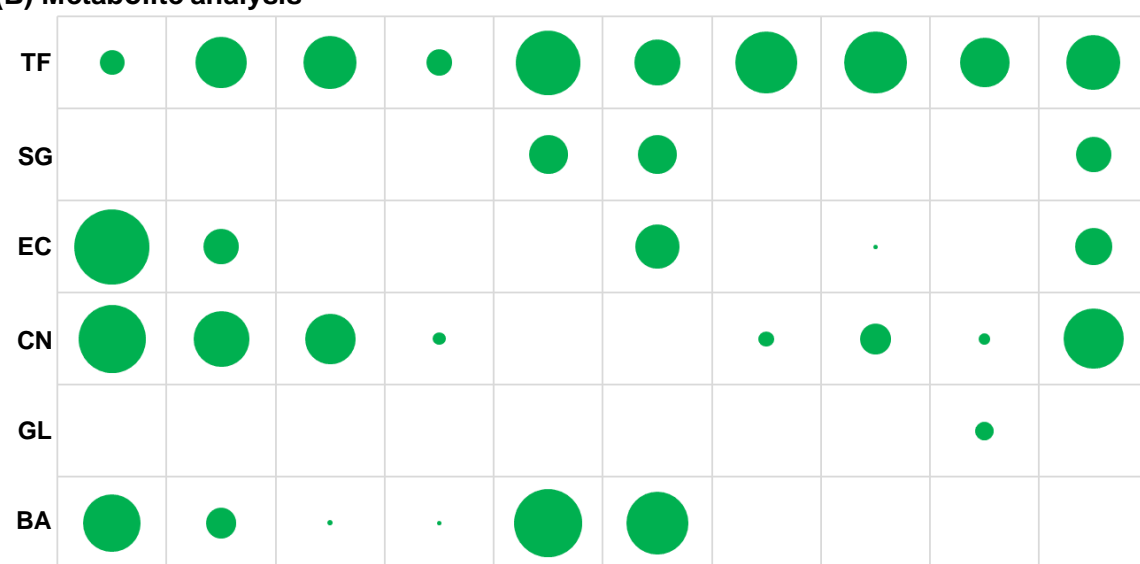


**Figure 4. *B. gladioli* antimicrobial activity and bioactive metabolite analysis.** **a** The bioactivity of metabolites extracts made from spent growth media from *B. gladioli* cultures. The bioactivity from equivalent metabolite extracts of strains representative of each clade are shown as follows (clade and BCC number are labelled): *B. gladioli* Clade 1A strain BCC1710, Clade 1B strain BCC1675, and Clade 1C strain BCC1678; *B. gladioli* Clade 2 strain BCC1731, *B. gladioli* pv. *allicola* reference Clade 2 strain BCC1645, and *B. gladioli* pv. *allicola* reference Clade 2 strain BCC1646; and *B. gladioli* Clade 3 strain BCC0238, *B. gladioli* pv. *agaricicola* reference Clade 3 strain BCC1883 (NCPPB 3852), and *B. gladioli* pv. *gladioli* reference Clade 3 strain BCC771 (LMG 2216<sup>T</sup>). Each area of bioactivity was cropped to scale and represents a 3 cm section of the inoculated petri dish. Zones of growth inhibition against *C. albicans* (**CA**), *R. mannitolilytica* (**RM**) and *S. aureus* (**SA**) are labelled as rows. **b** The quantitative analysis of known *B. gladioli* metabolites present in the metabolite extracts as determined by HPLC. Each circle is proportionally scaled to the mean peak height for the following metabolites: toxoflavin (**TF**), sinapigladioside (**SG**), enacyloxin IIA (**EC**), caryoynencin (**CN**), gladiolin (**GL**), and bongrekic acid (**BA**).

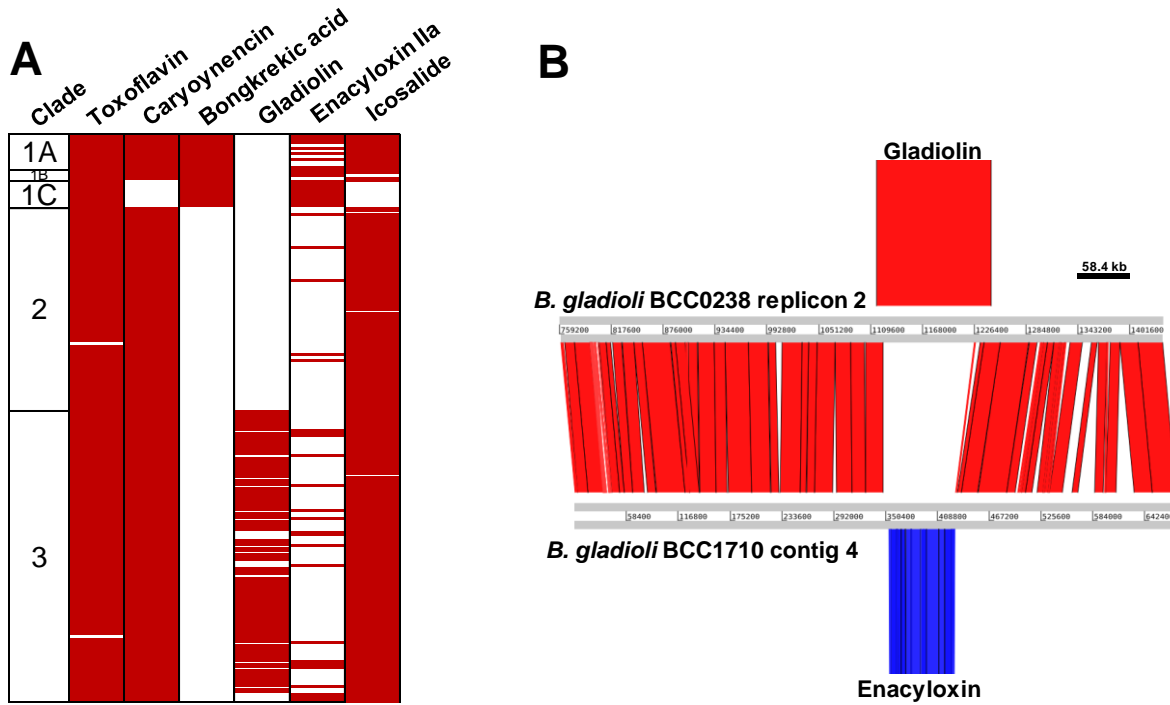


**Figure 5. Distribution of known *B. gladioli* specialized metabolite BGCs and common genomic location for gladiolin and enacyloxin biosynthesis.** **a** Sequence reads were mapped to known specialized metabolite BGCs to determine their presence or absence within the 206 the *B. gladioli* genomes. BGC presence indicated by red shading and columns from left to right show the *B. gladioli* clade, and BGCs for toxoflavin, caryoynencin, bongkrekic acid, gladiolin, enacyloxin Ila and icosalide. **b** A genomic comparison plot was constructed using the Artemis Comparison Tool for *B. gladioli* BCC0238 (clade 3) and BCC1710 (clade 1A). The common insertion point for either the gladiolin or enacyloxin BGCs in these strains is shown, together with extensive genomic synteny upstream and downstream of this specialized metabolite encoding location (scale bar indicates 58.4 kb).

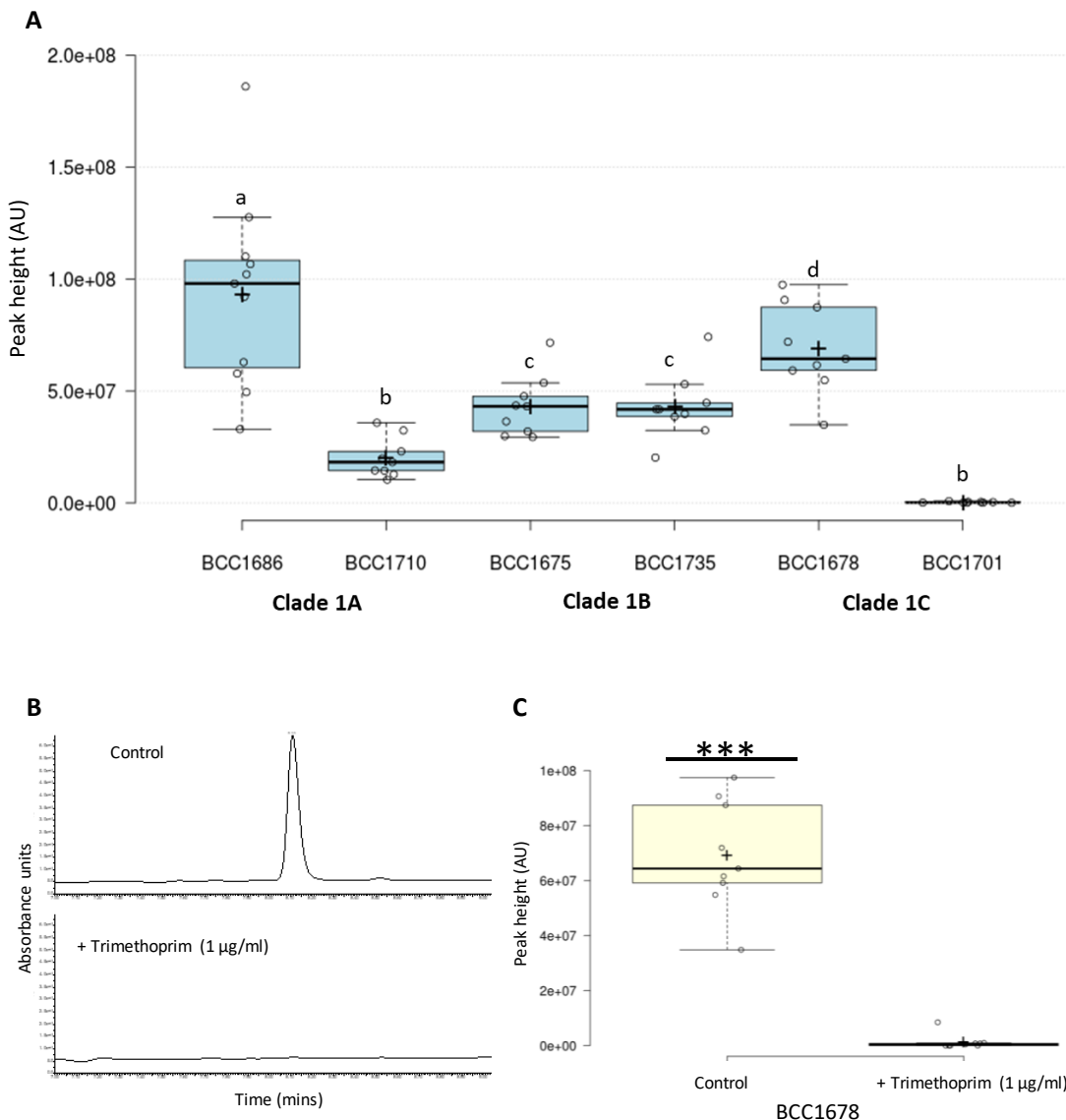


**Figure 6. Subinhibitory concentrations of trimethoprim reduce bongrekic acid production by *B. gladioli* clade 1 strains.** **a** HPLC analysis of 6 *B. gladioli* strains (strain numbers are shown) belonging to clades 1A, 1B and 1C demonstrated variable levels of bongrekic acid toxin production by HPLC analysis of their metabolite extracts (peak height is plotted). Differences between the mean values of bongrekic acid were determined using the LSD test  $\alpha=0.05$ . Means followed by the same letter are not significantly different. **b** The presence of subinhibitory concentrations of trimethoprim (1  $\mu$ g/ml) reduced the production of bongrekic acid in strain BCC1678 as shown the HPLC metabolite analysis comparing production levels against the control condition without antibiotic. **c** Quantitative comparison of bongrekic acid production by strain BCC1678 in the presence and absence of trimethoprim ( $n=9$ ) shows the significant ( $p<0.001$ ) suppression of toxin biosynthesis caused by antibiotic exposure. Statistical significance was determined using a two-tailed t-test.